Spin-up of ferrofluids: The impact of the spin viscosity and the Langevin function

Bruce A. Finlayson

Citation: Physics of Fluids (1994-present) **25**, 073101 (2013); doi: 10.1063/1.4812295
View online: http://dx.doi.org/10.1063/1.4812295
View Table of Contents: http://scitation.aip.org/content/aip/journal/pof2/25/7?ver=pdfcov
Published by the AIP Publishing

PHYSICS OF FLUIDS **25**, 073101 (2013)

Spin-up of ferrofluids: The impact of the spin viscosity and the Langevin function

Bruce A. Finlayson[a)]
Department of Chemical Engineering, Box 351750, University of Washington, Seattle, Washington 98195-1750, USA

(Received 13 August 2012; accepted 6 June 2013; published online 8 July 2013)

The spin-up of ferrofluids (rotational motion of a magnetic fluid induced by a rotating magnetic field) is examined computationally. Key questions are the impact of the spin viscosity, a mildly non-uniform magnetic field, and the importance of the Langevin magnetization equation. Comsol Multiphysics is used with boundary layer meshes to capture the effect when the spin viscosity is small. The effect of the spin viscosity is examined as it affects the critical magnetic field for non-rotational flow to occur and the magnitude of the rotational velocity and torque. Comparisons are made for the effect of magnetic field when using the Langevin magnetization equation and a linear equation. The equations for flow, magnetic field, and spin velocity are solved in two dimensions as a representation of a long cylinder with the magnetic field oriented perpendicular to the axis of the cylinder and rotated about that axis. Solutions are obtained for spin viscosities as low as 5.8×10^{-14} kg m s^{-1}. © *2013 AIP Publishing LLC*. [http://dx.doi.org/10.1063/1.4812295]

I. INTRODUCTION

A ferrofluid is a suspension of nano-sized magnetic particles, often magnetite, with a diameter of 10 nm. The particles are coated with a surfactant to prevent agglomeration, leading to a roughly spherical particle with a diameter up to 25 nm. They are suspended in either oil or water, giving rise to a fluid that flows and responds to magnetic fields. The spin-up phenomenon occurs when the ferrofluid is placed in a vertical cylinder and a magnetic field is oriented horizontally, and then rotated in that horizontal plane. This rotating magnetic field induces a rotary motion. Applications of ferrofluids include rotary seals in computer hard drives and in silicon manufacture, inertia dampers, and coolants in high-end loud speakers;[1] in microfluidic devices and nanodevices;[2,3] in displays,[4] heat pipes,[5] and electrical transformers.[6] They are also being examined for use in biomedical applications.[7,8]

The equations used to model the flow of ferrofluids include the Navier-Stokes equation augmented by body force terms from the magnetic field and new terms involving the spin velocity. The theories of Dahler and Scriven[9] and Condiff and Dahler[10] are used for a structured continua. They derive an equation governing the total angular momentum and then the internal angular momentum of the structure. This involves the spin velocity of the particles, which need not be the same as one-half the vorticity, which is the rotation rate of the fluid. Thus, the Navier-Stokes equations are augmented by a term involving the difference between those, and this term involves a new physical parameter called the vortex viscosity, which is only well established for infinitely dilute solutions. The spin velocity is determined by solving the equation for conservation of internal angular momentum, and this involves the diffusion or spread of spin velocity, with an appropriate parameter called the spin viscosity. Then the equation for magnetic field is affected by the spin velocity and vorticity, as well as the usual magnetic terms. While the concept of vortex viscosity is well established,[11] the

a)finlayso@uw.edu

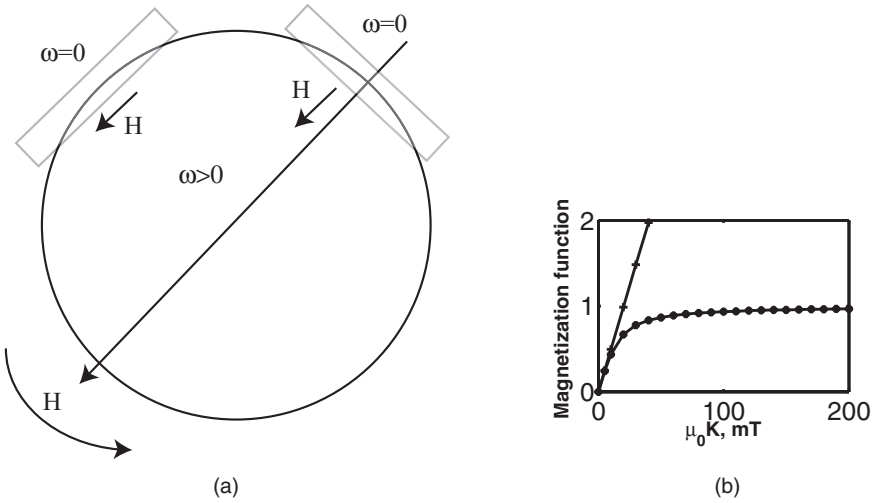

FIG. 1. (a) Geometry with rotating external magnetic field; (b) magnetization curve; • Langevin, + linear.

value of the spin viscosity is not known, and this has led to various interpretations of experimental phenomena, as discussed below. This paper provides a computational summary of the role of the spin viscosity and the conditions when it is important, or not.

Figure 1(a) shows the basic geometry and illustrates how the gradient of the spin velocity is aligned with the magnetic field in one area and is perpendicular to it in another area; the spin velocity is constant in the central region. The resulting complications are illustrated below. The magnetization of the ferrofluid depends upon the applied magnetic field, as shown in Figure 1(b). The differences caused by using the Langevin equation rather than a linear one are illustrated below.

The first observation of spin-up was by Moskowitz and Rosensweig.[12] They observed fluid rotation caused by the rotating magnetic field and measured the torque on a cylinder caused by the ferrofluid in a rotating magnetic field. Their observations of the flow, though, were made at a free surface since the ferrofluid is opaque. Later experimental and theoretical results[12–15] have shown that the flow at a free surface is influenced more by surface stresses than volume stresses, and the flow actually reverses direction at the free surface compared with the bulk fluid. Zaitsev and Shliomis[16] provided a theory for the spin-up phenomenon using the continuum theory of polar fluids developed by Dahler and Scriven.[9] At that time the equation was solved using a torque that was constant throughout the cylinder. There was no known value of spin viscosity, nor was the boundary condition on spin velocity known. The theoretical results did show, though, that the fluid rotated in almost solid body rotation, except near the wall. The fluid always rotated in the same direction as the magnetic field.

Kagan *et al.*[17] showed in a colloid suspension that flow reversal occurred as the magnetic field was increased, but his fluid used much larger particles than are usually found in ferrofluids. Later, Glazov[18,19] ascribed the motion to inhomogeneities in the magnetic field and higher harmonics in the applied magnetic field. Rosensweig's book[11] gives extensive information about ferrofluids, including a complete continuum theory involving the internal angular momentum equation and spin viscosity. He argued, as had Zaitsev and Shliomis,[16] that the spin viscosity, η', should depend upon the viscosity, η, and distance between the magnetic particles, l, which is the distance between the microeddy centers

$$\eta' \approx \eta l^2. \tag{1}$$

Feng *et al.*[20] made a similar argument. With this interpretation, the spin viscosity was in the range 10^{-17}–10^{-18} kg m s^{-1}. Rosensweig and Johnston[21] measured the velocity in an open container and found that the velocity exhibited solid body rotation except for a thin layer near the boundary (about 10% of the radius). Rosensweig *et al.*[13] showed that surface deflection would affect the direction of flow. This meant that observations at a free surface were not conclusive as to what was happening

in the bulk of the fluid. Rinaldi *et al.*[22] measured the torque on a completely filled cylinder with no free surface. They found that the magnitude of the torque increased as the magnetic field strength increased and as the frequency of rotation increased, so the presence of torque did not require a free surface. Chaves *et al.*[23] answered this question definitively by using ultrasound to measure the velocity in the bulk. Their Figure 3 shows that the azimuthal velocity is the same at levels one-fourth, one-half, and three-fourths of the height, but differs near the solid top surface. If they removed the top wall and had a free surface, they found that the velocity reversed direction at the top, but remained in the same rotation further down. Thus, the early work using the surface velocity to deduce motion in the cylinder is a misinterpretation. These measurements also give evidence that a two-dimensional theory is adequate to model the phenomena that occur in most of the cylinder.

Further support for Eq. (1) was provided by Travis and Evans.[24] They provided an analytical solution to the problem of axial flow of a ferrofluid in a cylindrical tube with no magnetic field applied and found that the spin viscosity led to sharp changes in the solution (compared with the solution of a non-ferromagnetic fluid) near the boundary of the tube. They then did molecular simulations and found a similar effect due to molecules being limited in their motion near the boundary.

Chaves *et al.*[25] presented an asymptotic theory and experimental measurements of the spin-up phenomenon. Their asymptotic theory identified the important terms in the equation and allowed simplification so that the zeroth-order and first-order solutions could be obtained analytically, for small magnetic fields. They then interpreted their ultrasound velocity measurements in terms of the theory and deduced that the spin viscosity was in the range 10^{-8}–10^{-12} kg m s^{-1}. This is a much larger value than predicted by Rosensweig[11] because the peak in rotational velocity occurred at about three-fourths of the radius, i.e., not forming a thin boundary layer at the wall. Thus, we are left with a discrepancy between estimates of the spin viscosity spanning 8–10 orders of magnitude. Khushrushahi and Zahn[26] used ultrasound to measure the velocity in a spherical cavity filled with ferrofluid when the magnetic field was rotating about a vertical axis. They also simulated that same situation using Comsol Multiphysics with a spin viscosity of 10^{-9} kg m s^{-1} and found that the predicted velocity was large enough that it should have been observable in the experiments, but no flow was measured. Experiments reported by Torres-Diaz *et al.*[27] in the same apparatus, but with the magnetic field oriented in a horizontal plane and carefully constructed to be uniform, measured a flow which was similar to that measured by Chaves *et al.*[25] although smaller. They also used the same apparatus but with a cylinder of ferrofluid instead of a sphere. In all these cases, they found that there was measureable flow; the peak in velocity was at a distance from the center of about three-fourths of the radius. They also redid earlier experiments[25,27] with a two-pole three-phase stator winding and found the same order of magnitude of velocity, thus indicating that inhomogeneities in the magnetic field were not the cause of the earlier experiments. Their conclusions are that the flows were similar in the spherical cavity and cylindrical container, the flow was rotational, and the flow magnitude increased with increasing magnetic field strength. Finally, they speculate that the effect is due to demagnetization effects of the finite height cylinder. Unfortunately, the magnetic field strength in these cases was not sufficiently high to induce irregular or reverse flow.

Shliomis *et al.*[28] argue that a possible reason for the rotation is that the magnetic field inside the cylinder is non-uniform, thus avoiding the need for a spin viscosity. They also postulate that the spin velocity causes a temperature increase, which in turn causes the magnetic field to be non-uniform inside the cylinder. These arguments are improved upon by Pshenichnikov *et al.*[29] The early work would lead to an estimated temperature rise of 0.6 K for the highest spin velocity reported below, but the later work, with a different estimate, leads to a estimated maximum temperature rise of 5 K.

Felderhof[30] considered a planar situation with vanishing force density and a uniform torque density. He[31] then solves the equations for flow velocity and spin velocity to second order in the applied uniform magnetic field, and based on that analysis concludes the large value of spin viscosity proposed by Chaves *et al.*[23,25] is not realistic. He extends the analysis for a cylinder,[32] still using the assumption that the magnetic field is small compared to the saturation magnetization so that the equations can be solved in a first-harmonic approximation. He finds that the analytical solution has a bifurcation as the magnetic field increases, and this leads to flow reversal. He[32] also says that no explanation exists for the flow reversal in the complete problem as the magnetic field is increased.

The analysis here is an extension that is not limited to small magnetic fields, and it does give flow reversal at large magnetic fields.

A central question is whether there is any need to include a spin viscosity in a theory that is relevant to observable phenomena. If a spin viscosity is included, the structured continuum approach of Dahler and Scriven[9] is necessary, and the stress tensor has an asymmetric portion. If not, the spin velocity equation can be rearranged (see below) so that the applied torque appears in the flow equation and it is unnecessary to have an asymmetric part of the stress tensor.

We are thus left with some contradictions for a closed cylinder. Both theory and experiment show that the velocity increases when the magnetic field is increased. Theory says that the velocity is smaller when the spin viscosity is smaller, other things being equal. Both theory and experiment also show that inhomogeneities in the magnetic field can cause irregular motion, but no experimental evidence exists that inhomogeneities cause regular, circular motion. In this paper, we will solve appropriate equations to show that:

- The velocity is smaller when the spin viscosity is smaller (as expected), and for the smallest estimated values of spin viscosity the velocity is negligible.
- The half-vorticity is a small fraction of the spin velocity for small spin viscosities.
- When the linear magnetization equation is used, reverse flow can occur when the magnetic field is increased, and the critical magnetic field for flow reversal is smaller for small spin viscosities. When the Langevin magnetization equation is used, however, reverse flow does not occur for the cases studied here.
- With an irregular magnetic field, it is easy to create irregular flow, but the flow is not circular.
- For the ferrofluid illustrated in Figure 1(b), the Langevin equation should be used for μ_0 $\times$ magnetic fields of 12.5 mT and larger.

II. DERIVATION OF EQUATIONS

A. Equations: Navier-Stokes, spin velocity, magnetic field

The equations are taken from Rosensweig[11] and are the same ones used in Finlayson[33] and Chaves *et al.*[25] The variables are velocity, pressure, spin velocity (of the magnetic particles), magnetic field, and magnetism. The Navier-Stokes equation is augmented by terms involving the asymmetric part of the total stress tensor and the magnetic body forces. When written in component form, the equations are for cylindrical geometry in a plane; the experiments of Chaves *et al.*[23] confirmed that this suffices for flow in a vertically oriented cylinder with a horizontal magnetic field, as long as one stays away from the top and bottom boundaries

$$\rho\frac{\partial \mathbf{v}}{\partial t}+\rho\mathbf{v}\bullet\nabla\mathbf{v}=-\nabla p+2\zeta\nabla\times(\boldsymbol{\omega}-\frac{1}{2}\nabla\times\mathbf{v})+\eta\nabla^2\mathbf{v}+\mu_0\mathbf{M}\bullet\nabla\mathbf{H}, \tag{2}$$

where ρ is the density (1030 kg m^{-3}), $\mathbf{v}$ is the velocity (m s^{-1}), t is time (s), p is pressure (Pa), ζ is the vortex viscosity (2.9×10^{-4} Pa s), $\boldsymbol{\omega}$ is the spin velocity (s^{-1}), η is the viscosity (4.5×10^{-3} Pa s), μ_0 is the permeability of free space (1.26×10^{-6} kg m (A s)$^{-2}$ = 1.26×10^{-6} N A^{-2}), $\mathbf{H}$ is the magnetic field (A m^{-1}, H in Oe $\times$ 1000/4π = H in A m^{-1}), $\mathbf{M}$ is the magnetization (A m^{-1}). The numerical values are appropriate for fluid EMG_900_2.[25] An alternative form is

$$\rho\frac{\partial \mathbf{v}}{\partial t}+\rho\mathbf{v}\bullet\nabla\mathbf{v}=-\nabla p+2\zeta\nabla\times\boldsymbol{\omega}+(\eta+\zeta)\nabla^2\mathbf{v}+\mu_0\mathbf{M}\bullet\nabla\mathbf{H}. \tag{3}$$

The spin velocity equation is

$$\rho I\frac{\partial \boldsymbol{\omega}}{\partial t}+\rho I\mathbf{v}\bullet\nabla\boldsymbol{\omega}=\mu_0\mathbf{M}\times\mathbf{H}+2\zeta(\nabla\times\mathbf{v}-2\boldsymbol{\omega})+\eta'\nabla^2\boldsymbol{\omega}, \tag{4}$$

where I is moment of inertia of one particle and η' is the spin viscosity (kg m s^{-1}). The spin equation is often simplified by assuming that the spin velocity adjusts instantaneously to the applied forces because moment of inertia, I, is so small. Since the particles are 25 nm in size, an estimate by

Schumacher *et al.*[34] gives I on the order of 10^{-16} m^2. Thus, we solve here

$$0 = \mu_0 \mathbf{M} \times \mathbf{H} + 2\zeta(\nabla \times \mathbf{v} - 2\boldsymbol{\omega}) + \eta' \nabla^2 \boldsymbol{\omega}. \tag{5}$$

The term for the pseudovector of the anti-symmetric stress[20] is

$$\mathbf{T}_x = 4\zeta \left(\frac{1}{2}\nabla \times \mathbf{v} - \boldsymbol{\omega}\right). \tag{6}$$

But if the spin viscosity η' is zero, the term in the momentum equation can be replaced by

$$2\zeta \nabla \times \left(\boldsymbol{\omega} - \frac{1}{2}\nabla \times \mathbf{v}\right) = \frac{\mu_0}{2}\nabla \times (\mathbf{M} \times \mathbf{H}) \tag{7}$$

and it is not necessary to consider an antisymmetric portion of the stress tensor. Note that if the magnetization and magnetic field are constant in space, then the curl is zero and there is no added term in the momentum equation.

The equation for magnetization is

$$\frac{\partial \mathbf{M}}{\partial t} + \mathbf{v} \bullet \nabla \mathbf{M} = \boldsymbol{\omega} \times \mathbf{M} - \frac{1}{\tau}(\mathbf{M} - \mathbf{M}_{eq}), \tag{8}$$

where τ is an "effective Brownian relaxation time that takes into account the effect of particle size polydispersivity";[25] $\tau = 1.9 \times 10^{-6}$ s. The magnetic equations are Maxwell's equations for a non-conducting material

$$\nabla \bullet \mathbf{B} = 0, \quad \nabla \times \mathbf{H} = 0, \quad \mathbf{B} = \mu_0(\mathbf{H} + \mathbf{M}), \tag{9}$$

where $\mathbf{B}$ is the magnetic flux density (T = N A^{-1} m^{-1}, 1 T = 10^4 G). Hence, we can take

$$\mathbf{H} = \nabla\phi, \quad \nabla^2\phi = -\nabla \bullet \mathbf{M}, \tag{10}$$

where ϕ is the magnetic potential (A). The equilibrium magnetization $\mathbf{M}_{\rm eq}$ is taken as the Langevin relation

$$\frac{\mathbf{M}_{eq}}{\phi_v M_d} = L(\alpha)\frac{\mathbf{H}}{|\mathbf{H}|} = \left[\coth(\alpha) - \frac{1}{\alpha}\right]\frac{\mathbf{H}}{|\mathbf{H}|}, \quad \alpha = \frac{\mu_0 M_d H V_c}{k_B T}, \tag{11}$$

where $\phi_{\rm v}$ is the volume fraction (0.043) and $M_{\rm d}$ is the domain magnetization (446 kA m^{-1}), $k_{\rm B}$ is the Boltzmann constant (1.38×10^{-23} J K^{-1}), T is the temperature (300 K), and $V_{\rm c}$ is the volume of the magnetic cores (1.37×10^{-24} m^3).

For small α, the Langevin formula reduces to $\alpha/3$.[35] In that case, Eq. (11) becomes

$$\frac{\mathbf{M}_{eq}}{\phi_v M_d} = \frac{\alpha}{3}\frac{\mathbf{H}}{|\mathbf{H}|} = \frac{\mu_0 M_d H V_c}{3k_B T}\frac{\mathbf{H}}{|\mathbf{H}|} = \frac{\mu_0 M_d V_c}{3k_B T}\mathbf{H}. \tag{12}$$

Combining terms, this gives

$$\mathbf{M}_{eq} = \frac{\mu_0 \phi_v M_d^2 V_c}{3k_B T}\mathbf{H} = \chi_i \mathbf{H}, \tag{13}$$

where the value of magnetic susceptibility χ_i is given by[11]

$$\chi_i = \frac{\mu_0 \phi_v M_d^2 V_c}{3k_B T}. \tag{14}$$

Here, we use a particle diameter of 1.377×10^{-8} m, slightly smaller than the 1.42×10^{-8} m listed by Chaves *et al.*,[25] in order that Eq. (14) gives $\chi_i = 1.19$ as listed by Chaves *et al.*[25] Comparisons are made below when using the Langevin Eq. (11) or the linear equation (13).

A demagnetization factor could be included to account for the reduction in magnetic field within the cylinder

$$\mathbf{H} = \frac{1}{1 + \chi_i/2}\mathbf{H}_{ext}. \tag{15}$$

Calculations of a steady magnetic field, uniform far from the cylinder, confirm that the equations above give the correct demagnetization factor. Here, we do not use the demagnetization factor so the magnetic field refers to the field inside the cylinder.

B. Boundary conditions

The boundary conditions on velocity are that the velocity is zero on the solid wall (a cylinder). The boundary condition on spin velocity is that it is zero on the wall. It was shown in Finlayson[33] that other boundary conditions (zero couple stress and spin velocity equal to one-half the vorticity) resulted in no velocity whatsoever. Solutions are also derived, though, for cases where the spin viscosity is zero; in that case the spin velocity equation is an algebraic equation and no boundary conditions are needed. Finlayson[33] showed that no flow occurred in that case either. Here, the investigation is enlarged to see the effect of non-uniformity of the magnetic field and higher harmonics when the spin viscosity is zero.

The boundary conditions on the magnetic variables are that the normal (**n**) component of the magnetic induction **B** is continuous across the boundary (i.e., the jump value is zero)

$$[\mathbf{n} \bullet \mathbf{B}] = 0 \tag{16}$$

and the tangential (**t**) component of magnetic field has zero jump across this boundary for a non-conducting fluid

$$[\mathbf{t} \bullet \mathbf{H}] = 0. \tag{17}$$

If the magnetic field is absolutely uniform far outside the cylinder, the boundary condition on the magnetic potential is

$$\phi = \phi_0[x \ \cos(\Omega_f t) + y \ \sin(\Omega_f t)], \tag{18}$$

where Ω_f is the radian frequency of oscillation, and the problem is only solved inside the cylinder. This is what was done in Finlayson[33] and Chaves *et al.*[25] However, experiments are done using a rotating magnetic field that is not absolutely uniform. Thus, simulations are done here using expressions like Eq. (18) but with higher harmonics.

C. Torque

One quantity that can be measured is the torque. The expression for torque is given by Chaves *et al.*[25]

$$\text{Torque} = \int_0^L \int_0^{2\pi} \left[\eta r^2 \frac{d}{dr}\left(\frac{v_\theta}{r}\right) + \zeta \frac{d}{dr}(r v_\theta) - 2\zeta r\omega + \eta' \frac{d\omega}{dr} \right] r d\theta \ dz|_{r=R}, \tag{19}$$

where r is the radial position (m), z is the height (m), v_θ is the azimuthal velocity (m s^{-1}), L is the height of the cylinder (0.0635 m), and R is the radius of the cylinder (0.0247 m). Expanding the terms and noting that the azimuthal velocity is zero on the boundary and the spin velocity is zero there, too, gives

$$\text{Torque} = \int_0^L \int_0^{2\pi} \left[\eta r^2 \frac{dv_\theta}{dr} + \zeta r^2 \frac{dv_\theta}{dr} + \eta' r \frac{d\omega}{dr} \right] d\theta \ dz|_{r=R}. \tag{20}$$

When the velocity is zero (or very small) and the spin velocity is constant in the cylinder (or the spin viscosity is zero), the torque is given by

$$\text{Torque} = -4\pi L R^2 \zeta \omega. \tag{21}$$

D. Non-dimensional equations for method 1

The equations are made non-dimensional by choosing a standard for each variable and defining a new non-dimensional value that is the original variable divided by that standard. Here, we will use two different methods. In the first method, only the magnetic terms are made non-dimensional. In the second method, used by Chaves *et al.*,[25] all terms are made non-dimensional in order to obtain a perturbation parameter, ε, and the inertial terms and time-dependent terms are ignored in the flow equation. The inertial terms are small and the velocity is interpreted as a velocity averaged over many cycles of the magnetic field, which is justified below when the magnetic field is not too large. The remaining terms are of the same order, which permits the perturbation method in ε.

The magnetic terms are made non-dimensional by choosing

$$\mathbf{H} = H_s\mathbf{H}', \ \mathbf{M} = M_s\mathbf{M}', \tag{22}$$

where $H_s = K$, where K is the strength of the applied magnetic field reduced by the demagnetization factor, and $M_s = \chi K$. Thus, in the discussion below, a value of $\mu_0 K = 12.5$ mT means the external magnetic flux density is $12.5\ (1+\chi_i/2) = 19.9$ mT.

Then the equations are (without the spin velocity time dependent terms)

$$\rho\frac{\partial \mathbf{v}}{\partial t} + \rho\mathbf{v}\bullet\nabla\mathbf{v} = -\nabla p + 2\zeta\nabla\times\boldsymbol{\omega} + (\eta+\zeta)\nabla^2\mathbf{v} + \mu_0\chi_i K^2\mathbf{M}'\bullet\nabla\mathbf{H}', \tag{23}$$

$$0 = \mu_0 K^2\chi_i\mathbf{M}'\times\mathbf{H}' + 2\zeta(\nabla\times\mathbf{v} - 2\boldsymbol{\omega}) + \eta'\nabla^2\boldsymbol{\omega}. \tag{24}$$

If $\eta' = 0$, then

$$2\zeta\ \nabla\times(\boldsymbol{\omega} - \frac{1}{2}\nabla\times\mathbf{v}) = \frac{\mu_0\chi_i K^2}{2}\nabla\times(\mathbf{M}'\times\mathbf{H}'), \tag{25}$$

$$\frac{\partial\mathbf{M}'}{\partial t} + \mathbf{v}\bullet\nabla\mathbf{M}' = \boldsymbol{\omega}\times\mathbf{M}' - \frac{1}{\tau}(\mathbf{M}' - \mathbf{M}'_{eq}), \tag{26}$$

$$\mathbf{H}' = \nabla\frac{\phi}{K}, \quad \nabla^2\frac{\phi}{K} = -\nabla\bullet\mathbf{M}', \tag{27}$$

$$M'_{eq} = \frac{M_{eq}}{\chi_i K} = \frac{\phi_v M_d}{\chi_i K}\left[\coth(\alpha) - \frac{1}{\alpha}\right]H'. \tag{28}$$

But

$$\frac{\phi_v M_d}{\chi_i K} = \frac{3}{\alpha} \tag{29}$$

so that the non-dimensional magnetization function is

$$\mathbf{M}'_{eq} = \frac{3}{\alpha}\left[\coth(\alpha) - \frac{1}{\alpha}\right]\mathbf{H}'. \tag{30}$$

For small α, this becomes

$$\mathbf{M}'_{eq} = \mathbf{H}'. \tag{31}$$

E. Non-dimensional equations for method 2

The equations can be further made non-dimensional (used in Sec. IV F only) following Chaves *et al.*[25] The additional dimensionless variables are

$$\mathbf{v}' = \mathbf{v}/v_s, \ x' = x/x_s, \ y' = y/x_s, \ t' = t/t_s, \ \boldsymbol{\omega}' = \boldsymbol{\omega}/\omega_s, \ p' = p/p_s \tag{32}$$

with $t_s = 1/\Omega_f$, where Ω_f is the radian frequency of oscillation of the magnetic field, $x_s = R_0$, the radius of the cylinder, and $y_s = R_0$. Choose

$$v_s = \frac{\mu_0 \chi_i K^2 \tilde{\Omega}_f R_0}{\zeta}, \ \omega_s = \frac{\mu_0 \chi_i K^2 \tilde{\Omega}_f}{\zeta} = \frac{v_s}{R_0}, \ \tilde{\Omega}_f = \Omega_f \tau, \ p_s = \frac{\eta v_s}{R_0}. \tag{33}$$

When these equations are inserted into the governing differential equations, and the resulting equations are rearranged, we get

$$\frac{\rho R_0^2 \Omega_f}{\eta} \frac{\partial \mathbf{v}'}{\partial t'} + \frac{\rho R_0^2 \Omega_f \mu_0 \chi_i K^2}{\zeta \eta} \mathbf{v}' \bullet \nabla' \mathbf{v}' = -\nabla' p' + 2\frac{\zeta}{\eta} \nabla' \times \boldsymbol{\omega}' + (1 + \frac{\zeta}{\eta}) \nabla'^2 \mathbf{v}' + \frac{\zeta}{\eta \tilde{\Omega}_f} \mathbf{M}' \bullet \nabla \mathbf{H}', \tag{34}$$

$$0 = \frac{1}{\tilde{\Omega}_f} \mathbf{M}' \times \mathbf{H}' + 2\nabla' \times \mathbf{v}' - 4\boldsymbol{\omega}' + \frac{\eta'}{\zeta R_o^2} \nabla'^2 \boldsymbol{\omega}', \tag{35}$$

$$\tilde{\Omega}_f \frac{\partial \mathbf{M}'}{\partial t'} + \frac{\mu_0 \chi_i K^2 \tilde{\Omega}_f \tau}{\zeta} \mathbf{v}' \bullet \nabla' \mathbf{M}' = \frac{\mu_0 \chi_i K^2 \tilde{\Omega}_f \tau}{\zeta} \boldsymbol{\omega}' \times \mathbf{M}' - (\mathbf{M}' - \mathbf{M}'_{eq}). \tag{36}$$

The following new parameters arise:

$$\frac{\eta'}{\zeta R_0^2}, \varepsilon = \frac{\mu_0 \chi_i K^2 \tau}{\zeta}, \frac{\zeta}{\eta}, \tilde{\Omega}_f, \chi_i, \frac{\rho R_0^2 \Omega_f}{\eta}, \frac{\rho v_s R_0}{\eta}, \alpha = \frac{\mu_0 M_d H V_c}{k_B T}. \tag{37}$$

As can be seen, the effect of magnetic field is always quadratic, and both it and the frequency of oscillation are important parameters. Another important parameter is

$$\kappa^2 = \frac{\eta}{\eta + \zeta} \frac{4 R_0^2 \zeta}{\eta'}. \tag{38}$$

The reason for this form of non-dimensionalization is that the parameter involving the magnetic field (ε) can be a perturbation parameter. When we use this form of the equations, we also neglect the time dependent and inertial terms in the momentum equation (34), as did Chaves *et al.*[25]

The expression for torque becomes

$$\text{Torque} = \eta v_s R_0 \int_0^L \int_0^{2\pi} \left[\left(1 + \frac{\zeta}{\eta} \right) \frac{dv'_\theta}{dr'} + \frac{\eta'}{\zeta R_0^2} \frac{\zeta}{\eta} \frac{d\omega'}{dr'} \right] d\theta \ dz|_{r=R} . \tag{39}$$

For these two-dimensional solutions, the integral over dz is just the height of the cylinder, ignoring end effects.

III. METHOD

The finite element method is used to solve the equations using Comsol Multiphysics, version 4.3. The velocity and pressure are represented by linear functions on each element, and the spin velocity, magnetic potential, and magnetization are represented by quadratic functions. The equations are solved in Cartesian coordinates, with u the velocity in the x direction and v the velocity in the y direction. The velocity and spin velocity are set to zero on the boundary of the cylinder. A convenient, and necessary, feature of Comsol Multiphysics is the ability to design boundary layer elements. These were done in sufficient density so that any boundary layers could be resolved without oscillations. This is especially important as the spin viscosity was decreased. For extremely small spin viscosities, Comsol Multiphysics no longer could be used since it represents the circular boundary as a series of straight lines and the whole phenomenon could be influenced by the small, but finite, corners in the boundary. However, before that happens, the essential physics is revealed.

The computations were speeded up by first solving with a coefficient of the velocity time derivative in the momentum equation that was smaller than it should be in order that the velocity

field in the center would be quickly established. Then the solution was continued with the correct time derivative using method 1 for about 16 cycles.

If the solution is started from zero using method 1, the velocity at the boundary is of course zero, but it almost instantaneously approaches its steady state value at the edge of a thin boundary layer. The velocity in the inner core (most of the domain at the onset) is still zero. Then the point at which the velocity is zero near the boundary gradually moves to the center until the flow is circular with a constant vorticity. The speed can be estimated by the analytical solution to Stokes first problem,

$$u = U_0 erfc(q), q = y/\sqrt{4\upsilon t}. \tag{40}$$

The edge of the boundary layer (for a 1% definition or $q = 1.8$) moves a distance of

$$y = 3.6\sqrt{\upsilon t} \tag{41}$$

and it would take 11 s for the boundary layer to move a distance equal to the radius of the domain. While this is a crude estimate because of the circular geometry, integrating this way to steady state would take a significant amount of time to reach steady state; in the terminology of differential equations the system is stiff with widely varying time constants. But steady state can be reached much faster if one uses the two-step process. In the second step, the calculations were done long enough to observe the steady state.

IV. RESULTS

In the simulations reported below, the parameters are representative of the oil-based ferrofluid EMG_900_2 as presented by Chaves *et al.*[25] The parameters that change are the spin viscosity, strength of the magnetic field, frequency, and magnetization equation, which are reported for each case.

A. Demagnetization factor

A sample problem is solved first to insure that the magnetic field is correct. Consider a square on which the magnetic potential on one side is 1.0 and on the opposing side it is 0. On the top and bottom the flux is zero. Put a circle at the center and have it represent a magnetic material with a magnetic susceptibility of 1.0. An analytical solution exists for this problem,[36] and the potential on the boundary of the circle is plotted in Figure 2. This shows that the numerical solution is the same as the analytical solution for the magnetic potential, ϕ, on the circle. This solution is derived using the linear magnetization equation (13).

B. Perturbation solution

Chaves *et al.*[25] provide a perturbation solution to these equations when the magnetic field is small (small ε). They provide a zeroth order and first order perturbation solution. The numerical

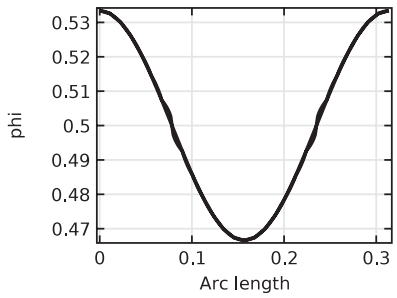

FIG. 2. Comparison of the magnetic potential on the circle for two solutions, one an analytical solution $[0.5 + 0.05 \times (2/3)\cos(\theta)]$ and the other a numerical solution for demagnetization of a circle when $\chi = 1$.

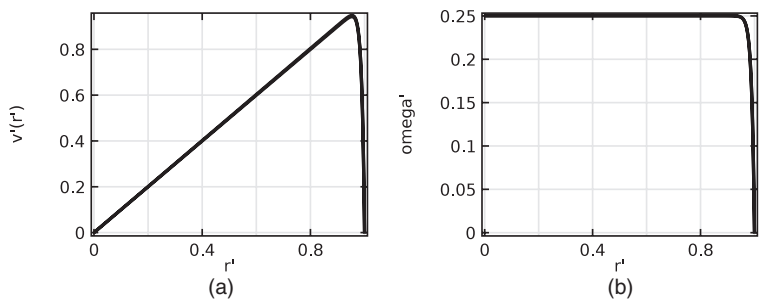

FIG. 3. Comparison of numerical and zeroth-order perturbation solution; (a) velocity along the line $y = 0$; (b) spin along the line $y = 0$.

solution can be compared with the zeroth order perturbation solution to validate the equations. The only change in the program is to set the ε parameter to zero and use $\mathbf{M'}_{eq} = \mathbf{H'}$. The analytical solutions are

$$v'_\theta = \frac{\zeta}{2\kappa\eta^*(1+\tilde{\Omega}_f^2)}\frac{I_1(\kappa)}{I_0(\kappa)}\left[r' - \frac{I_0(\kappa r')}{I_1(\kappa)}\right], \eta^* = \eta + \zeta\frac{I_2(\kappa)}{I_1(\kappa)}, \tag{42}$$

$$\omega'_z = \frac{\eta+\zeta}{4\eta^*(1+\tilde{\Omega}_f^2)}\left[1 - \frac{I_0(\kappa r')}{I_1(\kappa)}\right]. \tag{43}$$

The Bessel functions are quite large, and take the following values for $\kappa = 100$:

$$\mathrm{I}_0(100) = 1.0738 \times 10^{42}, \quad \mathrm{I}_0(95.4) = 1.105 \times 10^{40}, \quad \mathrm{I}_1(100) = 1.0684 \times 10^{42}, \quad \mathrm{I}_2(100) = 1.0524 \times 10^{42}. \tag{44}$$

For the parameters used, the coefficients are $0.995 \times 1.01 \times 10^{-3}$ for velocity and 0.25 for spin velocity. The peak velocity is obtained in the zeroth order perturbation solution at $r' = 0.954$, where the peak velocity is 0.949×10^{-4}. The peak spin velocity is of course 0.25. The zeroth order perturbation solution and numerical solution (using method 2) are plotted in Figures 3(a) (velocity) and 3(b) (spin velocity). Note the boundary layer is well resolved. The dimensionless spin velocity takes the value 0.25 over most of the domain, whereas one-half the dimensionless vorticity is 10^{-3}; thus, most of the angular momentum is concentrated in the spin rather than the vorticity. The numerical and analytic values of the non-dimensional torque $\mathbf{M'} \times \mathbf{H'}$ (which is constant in the cylinder) are 1.12×10^{-3} and 1.11×10^{-3}, showing good agreement. The value $\kappa = 100$ here corresponds to $\eta' = 6.65 \times 10^{-11}$ kg m s^{-1} for the magnetic fluid treated here.

C. Base case, with a large spin viscosity

The first case uses a large spin viscosity ($\eta' = 5.8 \times 10^{-10}$ kg m s^{-1}) and $\mu_0 K = 12.5$ mT so that the effects near the boundary can be easily observed. The graded mesh is shown in Figure 4(a). The streamlines are shown in Figure 4(b), and the flow is circular. The extent of the boundary layers is demonstrated in Figure 4(c); this is the vertical velocity along the line $y = 0$, and the profile is plotted at 41 different times; obviously it does not change in time. In the supplementary material, Figure S1[37] shows one component of the magnetization. This component is constant over most of the domain, but has variations in the boundary layer. This region, shown in the non-red colors, rotates as the magnetic field rotates. Figure S2[37] shows the magnitude of the Langevin function, which is constant over most of the domain except for a thin boundary layer where the magnetic field also varies. These two figures illustrate the impact of having the spin velocity gradient be parallel or perpendicular to the magnetic field, as seen in Figure 1(a).

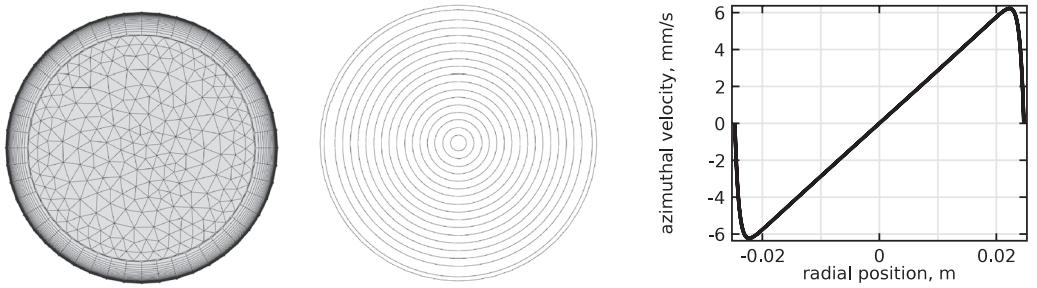

FIG. 4. Solutions with spin viscosity $= 5.8 \times 10^{-10}$ kg m s^{-1} and $\mu_0 K = 12.5$ mT; (a) graded mesh; (b) streamlines; (c) vertical velocity v along line $y = 0$.

D. Effect of magnetic field and spin viscosity

Calculations were made for spin viscosities of $\eta' = 5.8 \times 10^{-8}$, $\eta' = 5.8 \times 10^{-10}$, $\eta' = 5.8 \times 10^{-12}$, $\eta' = 5.8 \times 10^{-14}$ kg m s^{-1} and values of $\mu_0 K$ as high as 1600 mT. The results are shown in Table I (at 12.5 mT) and plotted in Figure 5(a). As the magnetic field increases, the torque also increases, up to a point, and then it starts to level off.

Solutions are given in Figures 5(b) and 5(c) for the same magnetic field (μ_0K = 12.5 mT) and spin viscosities 100 and 10 000 times smaller than that for Figure 4(c). Figure 5(b) is for $\eta' = 5.8 \times 10^{-12}$ and plots the azimuthal velocity along lines $y = 0$, $x = 0$, and $y = x$; the curves superimpose. Figure 5(c) is for $\eta' = 5.8 \times 10^{-14}$ kg m s^{-1}. The vertical velocity is smaller for smaller spin viscosities, and the boundary layer becomes thinner. The vorticity is easily deduced from these figures. It is constant in the central core but varies (and changes sign) in a thin region near the boundary. Table I indicates that the half-vorticity is much smaller than the spin velocity, and becomes a smaller and smaller fraction as the spin viscosity decreases. One might suspect that the velocity is not computed accurately near the boundary, but Figure 5(d) is an exploded view near the boundary. Clearly, there are no ambiguous oscillations from node to node, although the velocity is starting to vary with time near the boundary. This cyclic oscillation can be seen in Figure S3 in the supplementary material.[37]

Figure 5(e) shows the vertical velocity when the spin viscosity is 5.8×10^{-12} kg m s^{-1}, and the magnetic field is higher ($\mu_0 K = 1$ T), high enough to cause the velocity near the boundary to begin to vary in time. For these parameters, it is necessary to use the full equations with the time derivative of velocity and the inertial terms, as has been done in all Figures 4 and 5. The streamlines are shown in Figure 5(f).

For the cases shown in Figure 5(a), the flow is always counterclockwise. Figure 5(g) shows the initial time development of the flow for 60 T, and the flow was circular and counterclockwise. It is shown below that clockwise flow (i.e., flow reversal) can occur when the linear magnetization equation is used.

TABLE I. Comparison of solutions with different spin viscosities at $\mu_0 K = 12.5$ mT.

η'	kg m s^{-1}	5.80E-08	5.80E-10	5.80E-12	5.80E-14
max. v	mm s^{-1}	21.0	6.24	0.699	0.072
0.5*vorticity at center	s^{-1}	1.85	0.29	0.029	0.01
min. half-vorticity	s^{-1}	− 2.85	− 5.06	− 5.36	− 5.42
max spin	s^{-1}	75.8	88.9	91.2	91.4
torque	μNm	− 12.9	− 12.6	− 12.5	− 12.6

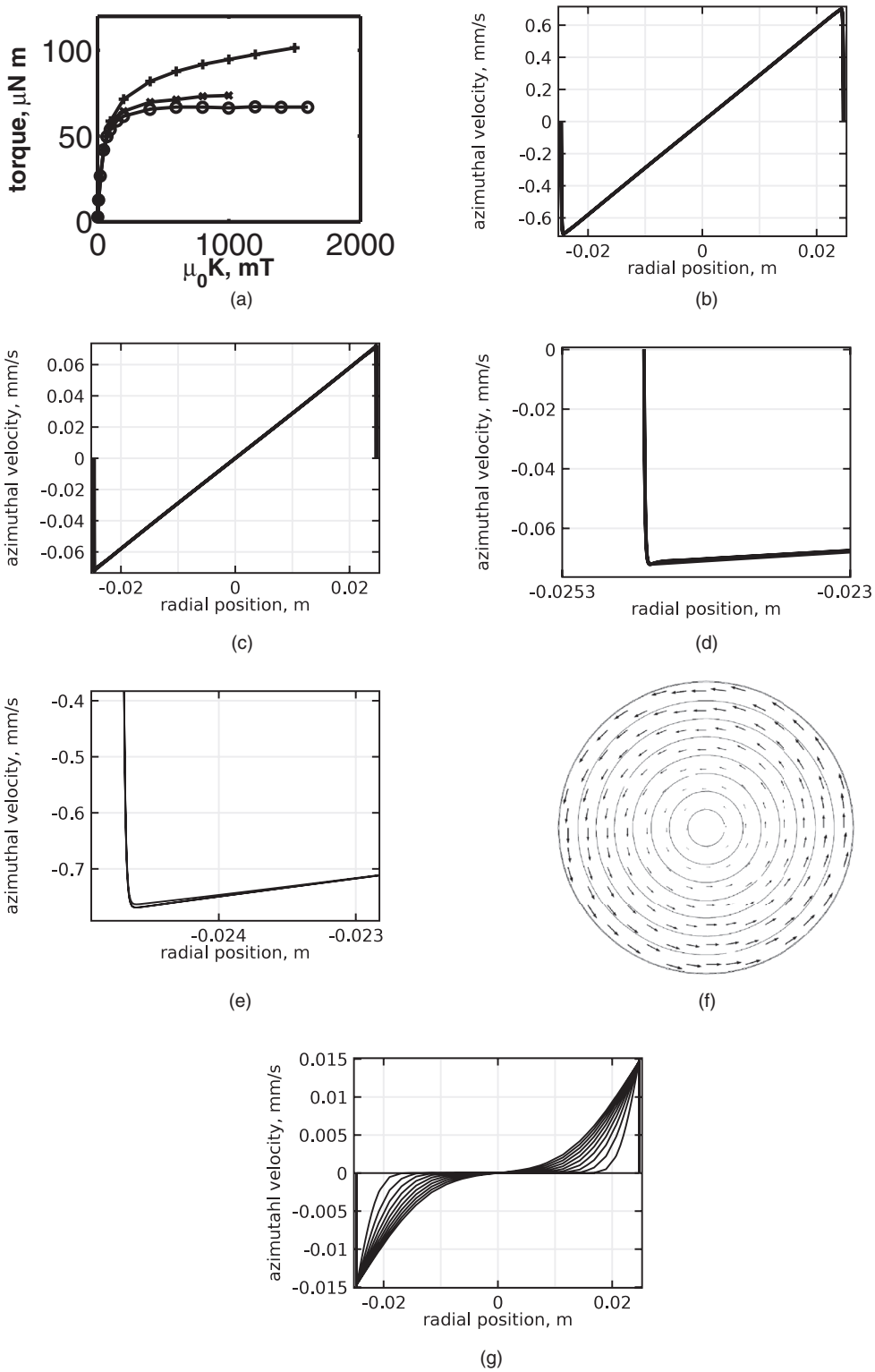

FIG. 5. Effect of spin viscosity and applied field: (a) torque vs. $\mu_0 K$ for fluids with different spin viscosities; spin viscosity $= +5.8 \times 10^{-10}$ kg m s^{-1}, $\times\, 5.8 \times 10^{-12}$ kg m s^{-1}, $\bullet\, 5.8 \times 10^{-14}$ kg m s^{-1}; (b) spin viscosity $= 5.8 \times 10^{-12}$ kg m s^{-1} and $\mu_0 K = 12.5$ mT, azimuthal velocity along lines $y = 0$, $x = 0$, $y = x$; (c) spin viscosity $= 5.8 \times 10^{-14}$ kg m s^{-1} and $\mu_0 K = 12.5$ mT, azimuthal velocity along lines $y = 0$, $x = 0$, $y = x$; (d) enlargement of (c); (e) spin viscosity $= 5.8 \times 10^{-12}$ kg m s^{-1} and $\mu_0 K = 1000$ mT, vertical velocity along line $y = 0$; (f) streamlines for case (e); (g) transient case from $t = 0$ to 8 for spin viscosity $= 5.8 \times 10^{-14}$ kg m s^{-1} and $\mu_0 K = 60$ T, vertical velocity along line $y = 0$.

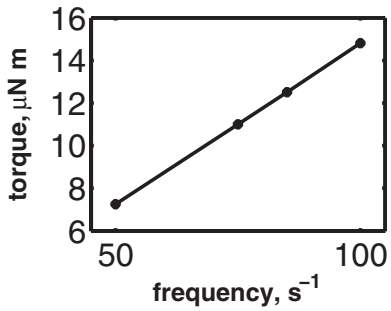

FIG. 6. Torque vs. frequency for spin viscosity $= 5.8 \times 10^{-12}$ kg m s^{-1} and $\mu_0 K = 12.5$ mT.

E. Effect of frequency

The effect of frequency is shown in Figure 6 and Table II for a spin viscosity of $\eta' = 5.8 \times 10^{-12}$ kg m s^{-1} and $\mu_0 K = 12.5$ mT. As the frequency is increased, the torque increases as well.

F. Solutions without inertial terms or velocity time derivatives: Method 2

Solutions obtained without the inertial terms or velocity time derivatives are shown in Figures 7(a)–7(c) for the three spin viscosities. These figures are for the same cases as shown in Figures 4(c), 5(b), and 5(c). The solution is generally the same within two significant figures as long as the flow does not reverse direction. Numerical values are provided in Table III.

G. Examination of the adequacy of the mesh

For the case $\mu_0 K = 12.5$ mT and spin viscosity 5.8×10^{-12} kg m s^{-1}, several cases were calculated using meshes with successively more dense meshes, using method 1. The boundary layer meshes are established by choosing the width of the first one, the ratio between them, and how many layers are formed. The starting values, ratios, number of layers, total width of the boundary layer mesh, total number of elements (in the total domain), and total degrees of freedom are listed in Table IV. For the three cases, the results for peak velocity (0.701, 0.692, 0.699 mm s^{-1}), peak spin velocity (88.4, 90.8, 91.2 s^{-1}), and torque (-11.6, -12.4, -12.5 μN m) were close, indicating the accuracy of the calculations.

H. Results with zero spin viscosity

The problem was solved using a zero spin viscosity and calculating the spin velocity from Eq. (5); $\mu_0 K$ was taken as 12.5 mT. The velocity was extremely small, 10^{-9} mm s^{-1}, so that it is essentially zero. The spin velocity (averaged over time) was about the same, 90.8 s^{-1} vs. 88.4–91.2 depending upon the mesh for the case with a spin viscosity $= 5.8 \times 10^{-12}$ kg m s^{-1}. This time the torque is constant in the cylinder and the only term in Eq. (19) that is non-zero is the one involving spin velocity, which is constant in the domain. The torques are comparable (-12.8 vs. -12.5 μN m). The problem can be reformulated (in Comsol) to leave out the velocity all together, and the spin

TABLE II. Effect of frequency; $\mu_0 K = 12.5$ mT, $\eta' = 5.8$e-12 kg m s^{-1}.

frequency	Hz	50	75	85	100
max. v	mm s^{-1}	0.407	0.617	0.699	0.82
0.5*vorticity at center	s^{-1}	0.0170	0.026	0.029	0.035
max spin	s^{-1}	51.8	75.8	91.2	106.6
torque	μNm	− 7.26	− 11	− 12.5	− 14.8

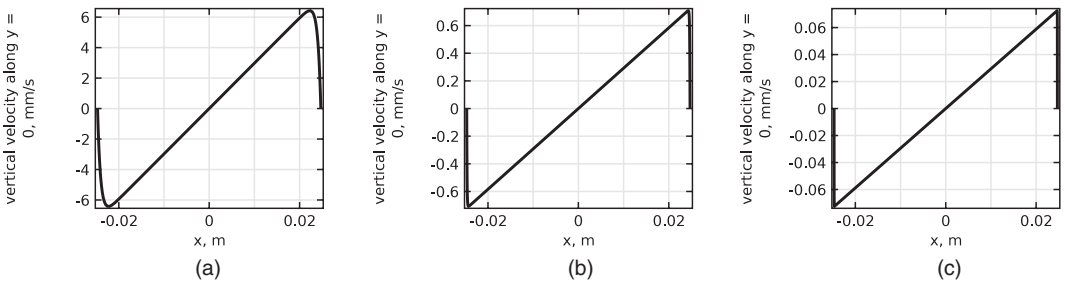

FIG. 7. Solutions obtained by ignoring the inertial terms and velocity time derivative, $\mu_0 K = 12.5$ mT; spin viscosity = (a) 5.8×10^{-10} kg m s^{-1}, (b) 5.8×10^{-12} kg m s^{-1}, (c) 5.8×10^{-14} kg m s^{-1}.

velocity and torque are almost the same (89.5 s^{-1} and -12.7 μN m). The same problem (without a velocity) can be solved in MATLAB since only ordinary differential equations are involved. This gives 89.2 s^{-1} and -12.6 μN m.

I. Effect of non-homogeneous magnetic field

The magnetic field was changed to simulate a case in which higher harmonics are included by the electric current generating the magnetic field. The base case uses the following boundary conditions for magnetic potential and a spin viscosity of 5.8×10^{-12} kg m s^{-1}:

$$\text{Base case}: \quad \frac{\phi}{K} = x\ \cos(\Omega_f t) + y\ \sin(\Omega_f t). \tag{45}$$

Simulations were done using the following potentials and magnetic fields:

$$\text{Case 1}: \quad \frac{\phi}{K} = x\ [\cos(\Omega_f t) + 0.05\ \cos(2\Omega_f t) + 0.005\cos(3\Omega_f t)] + y\ [\sin(\Omega_f t) + 0.05\ \sin(2\Omega_f t) + 0.005\sin(3\Omega_f t)],\ \mu_0 K = 12.5\,\text{mT}, \tag{46}$$

$$\text{Case 2}: \quad \frac{\phi}{K} = x\ [\cos(\Omega_f t) + 0.05\ \cos(2\Omega_f t + \pi/4) + 0.005\cos(3\Omega_f t + \pi/2)] + y\ [\sin(\Omega_f t) + 0.05\ \sin(2\Omega_f t + \pi/4) + 0.005\sin(3\Omega_f t \pi/2)],\ \mu_0 K = 12.5\,\text{mT}, \tag{47}$$

$$\text{Case 3}: \quad \frac{\phi}{K} = x\ \cos(\Omega_f t) + (0.1/3)[x\ \cos(\Omega_f t)]^3 + y\ \sin(\Omega_f t) + (0.1/3)[y\ \sin(\Omega_f t)]^3,\ \mu_0 K = 12.5\,\text{mT}, \tag{48}$$

$$\text{Case 4}: \text{Case 2 with} \quad \mu_0 K = 50\,\text{mT}. \tag{49}$$

TABLE III. Comparison of solutions with Methods 1 and 2; $\mu_0 K = 12.5$ mT, 85 Hz.

	inertial terms:	with	without	with	without	with	without	with	without
η'	kg m s^{-1}	5.80E-08	5.80E-08	5.80E-10	5.80E-10	5.80E-12	5.80E-12	5.80E-14	5.80E-14
max. v	mm s^{-1}	21.0	21.5	6.24	6.43	0.692	0.708	0.072	0.072
0.5*vorticity at center	s^{-1}	1.85	1.92	0.29	0.3	0.029	0.029	0.010	0.003
min. half-vorticity	s^{-1}	− 2.87	− 3.05	− 5.06	− 5.34	− 5.32	− 5.41	− 5.42	− 5.41
max. spin	s^{-1}	75.7	82.2	88.9	93.1	90.8	90.3	91.4	90.9
torque	μNm	− 13.0	− 13.8	− 12.6	− 13.1	− 12.4	− 12.6	− 12.6	− 12.6

TABLE IV. Mesh characteristics for graded meshes.

First element (fraction of R)	Ratio	Number of layers	Width of boundary layer mesh (fraction of R)	Number of elements	Degrees of freedom
2.7e-4	1.15	30	0.117	1986	32,818
5e-5	1.2	38	0.255	2370	40,114
1e-5	1.2	46	0.219	2754	47,410

Results with $\mu_0 K = 12.5$ mT were (case: base, 1, 2, 3): peak velocities of 0.699, 0.706, 0.715, 0.700 mm s^{-1}, respectively, and spin velocities of 91.2, 104, 102, and 88.8 s^{-1}, respectively. The respective torques were -12.5, -13.6, -13.8, and -12.4 μN m. Results with $\mu_0 K = 50$ mT were (case: base, 4): peak velocities: 1.69, 1.73 mm s^{-1}; spin velocities: 304 and 315 s^{-1}; and torques: -42.8 and -43.8 μN m. For cases 1–4, the flow was still quite circular except near the boundary, where it oscillated due to the changing magnetic potential. In case 4, the torque and spin velocity oscillated with time, and the values given are averages over 10 time points.

The base case ($\mu_0 K = 12.5$ mT) and case 2 were also run with zero spin viscosity and no velocity. The average spin velocities were: 89.5 and 89.8 s^{-1}, respectively, and the respective torques were both -12.7 μN m. For case 2, the torque and spin velocity, while constant in space, oscillated in time and these values are averages over 99 time points; the spin velocity oscillated smoothly between 80 and 105 s^{-1}. Using MATLAB to solve the equations as ordinary differential equations gave 89.3 s^{-1} and -12.6 μN m. This solution (Figure 8) would be the more accurate one because the tolerances for solving the ordinary differential equations can be very small. The same was done for a base case ($\mu_0 K = 50$ mT) and case 4, which gave the results: spin velocities of 308 s^{-1} for both cases, and torques of -43.4 and -43.5 μN m. In this case, only MATLAB was used with very strict tolerances because the problem was too unstable to solve as partial differential equations in Comsol. In summary, with irregular boundary conditions, the spin velocity can oscillate in time, but the average values are almost the same.

Solutions (using method 2) were obtained by Torres-Diaz and Rinaldi[38] for a multipole magnetic field as would be generated by an electric motor, but under the assumption that the time dependence is averaged, the effect of velocity is negligible in the magnetization equation, the magnetic field $\mu_0 K$ is from 2 to 12 mT, and the spin viscosity is 12×10^{-10} kg m s^{-1}. The equations for the magnetic field were solved analytically for the linearized magnetization equation. The solutions for a cylinder are similar to those in Chaves *et al.*[25] in that substantial velocities are obtained, necessitating a large spin viscosity.

J. Effect of linear magnetization equation

The results using the Langevin magnetization equations (11) and (28) can be compared with results using linear magnetization equations (13) and (31). Results for the former are in Table I. For

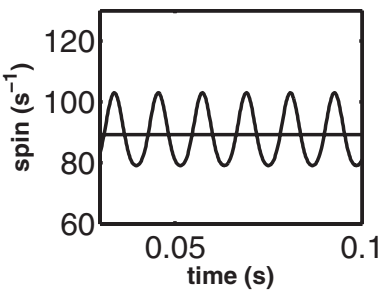

FIG. 8. Spin when there is no spin viscosity or velocity. Straight line is for the base case and the oscillating curve is for case 2. $\mu_0 K = 12.5$ mT.

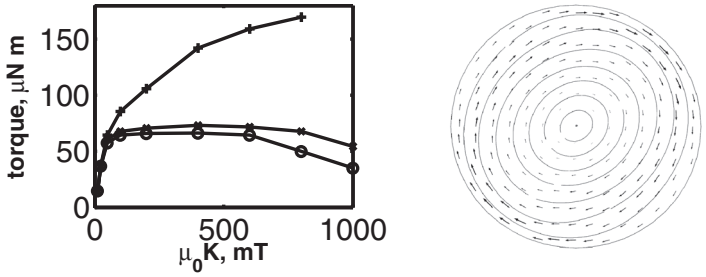

FIG. 9. Effect of spin viscosity and applied field for a linear magnetization curve; (a) torque vs. $\mu_0 K$ for fluids with spin viscosity $= +5.8 \times 10^{-10}$ kg m s^{-1}, $\times\, 5.8 \times 10^{-12}$ kg m s^{-1}, o 5.8×10^{-14} kg m s^{-1}; (b) streamlines showing flow reversal for spin viscosity $= 5.8 \times 10^{-14}$ kg m s^{-1} and $\mu_0 K = 1000$ mT.

a spin viscosity of 5.8×10^{-12} kg m s^{-1} and $\mu_0 K = 12.5$ mT, the ratio of the magnetization function for the linear case to the Langevin case is 1.21. The ratio of the results (as shown in Table I) is from 1.15 to 1.18. When $\mu_0 K$ is reduced to 5 mT, the ratio of magnetizations functions is 1.10, whereas the ratio of the results ranges between 0.98 and 1.05. When $\mu_0 K$ is reduced to 2.5 mT, the ratio of magnetizations functions is 1.01, whereas the ratio of the results ranges between 1.00 and 1.01. Thus, when the magnetic field is small enough, the results using the Langevin equations (11) and (28) asymptotically approach those found when using the linear equations (13) and (31).

Since the linear magnetization equation results in a much larger magnetization than does the Langevin equation, it is expected that effects occur at lower magnetic field when the linear equation is used. For a particular spin viscosity, as the magnetic field is increased the torque increases to a maximum and then starts to decrease (Figure 9(a)). When the magnetic field is increased even further the flow becomes time dependent, and eventually the circular pattern of the streamlines turns into a figure eight; for further increases in magnetic field the flow direction reverses, and eventually the streamlines become circular in the reverse direction (Figure 9(b)). This flow reversal does not happen when the Langevin magnetic equation is used for $\mu_0 K$ up to 60 T, which is extremely high. This is presumably because the magnetization has reached a saturated value, as shown in Figure 1(b).

It is difficult to identify one critical magnetic field that characterizes reverse flow since the flow first becomes not quite circular, then breaks into four vortices, two of them small near the boundary in reverse flow, and only for large $\mu_0 K$ does one get reverse flow in most of the domain. However, with that caveat, the results in Figure 9(a) are an indication that the point at which the torque vs. magnetic flux density curve peaks is strongly affected by the spin viscosity. That "critical" field is smaller for smaller spin viscosities. This is comparable to the bifurcations predicted by Felderhof[32] for a simplified model. Felderhof[32] uses a parameter that is the square root of ε to define the magnetic fields at which bifurcation is predicted, and the bifurcations occur at about $\varepsilon = 64$; for the fluid treated here, this is $\mu_0 K = 100$ mT. That is also near the point at which the torque vs. magnetic field curve peaks for the smallest spin viscosity (see Figure 9(a)). But Felderhof[32] does this analysis for $\eta'/(\eta R^2) = 0.3$, whereas values used here are for 3.28×10^{-3}, 3.28×10^{-5}, and 3.28×10^{-7}. For the analysis here, with that parameter $= 0.3$, the critical magnetic field would be above $\mu_0 \mathrm{K} = 600$ mT. Nonetheless, the comparison is intriguing since Felderhof's[32] analysis is made assuming certain terms are small, whereas in the analysis here all terms are included.

K. Comparison with experimental trends

The limited experimental data for closed cylinders indicates that the torque increases with magnetic field,[21] as predicted here. But the ultrasound measurements of Khushrushahi and Zahn[26] measure no velocity when the ferrofluid is contained within a sphere (with no free surface) and a uniform magnetic field is rotating. If the spin viscosity had been as high as 10^{-8} kg m s^{-1}, a measureable flow was predicted. If the spin viscosity is 10^{-18} kg m s^{-1}, then no flow should have

been observed, as was the case. More recently, Torres-Diaz *et al.*[27] use ultrasound techniques to measure the velocity in fully contained spheres and cylinders and find a measureable velocity. They suggest the mechanism is either a demagnetization effect, a spin viscosity effect, or some other, unknown, effect.

The computational results shown here, for a closed cylinder, mirror the experimental results seen for cylinders with a free surface:[12–15,21–23,25,26] torque increasing with magnetic field, torque increasing with frequency, flow reversal above a critical magnetic field, solid body rotation except for a thin boundary layer near the cylinder wall. Unfortunately, the literature suggests that when there is a free surface, the phenomenon is controlled by the free surface; experiments by Chaves *et al.*[23] indicate that this is certainly true at the top of an open cylinder, although the analysis here might apply at lower elevations away from the surface. It is interesting to speculate about what happens for even smaller spin viscosities than those used here (10^{-14} kg m s^{-1}). The critical magnetic field would be lower, and perhaps in the range for which the linear magnetization is valid, and flow reversal could occur. The velocity, though, would be very small, since it decreases as the spin viscosity decreases.

V. CONCLUSIONS

The numerical calculations were performed with the finite element method, but it is necessary to use a mesh composed of boundary layers near the outer boundary of the ferrofluid. The spin velocity and half-vorticity are nearly constant in the central core, but vary in a thin boundary layer. For moderate magnetic fields, the flow field represents a solid body rotation, except for a small region near the boundary. For small spin viscosity, the half-vorticity is a small fraction of the spin velocity.

Simulations show that for a given spin viscosity and a linear magnetization equation, as the magnetic field is increased the flow becomes irregular and reverses direction. This is suggestive of the bifurcations predicted by Felderhof.[32] The critical magnetic field at which this happens decreases as the spin viscosity decreases, at least for the linear magnetization equation (13). When using the Langevin magnetic equation, flow reversal is not observed for the parameters used here. If the spin viscosity is zero, no flow is predicted when the magnetic field is uniform. To get circular velocity streamlines, it is necessary to have a uniform magnetization, a non-zero spin viscosity, and a magnetic field below a critical value. If the magnetic field is inhomogeneous, then irregular flow occurs in any case; it also occurs if the magnetic field is high, but "high" depends upon the spin viscosity and the magnetization equation.

If the spin viscosity is really as small as 10^{-18} kg m s^{-1}, the phenomenon studied here has no meaning for experiments that have been done heretofore. The predicted velocity is much smaller than has been measured and the predicted flow would be irregular for the magnetic field strengths used even if the magnetic field is uniform. Thus, the spin-up of ferrofluids cannot be used as an example requiring a non-symmetric portion of the stress tensor. This analysis and comparison is not relevant to a case with a free surface, though.

[1] K. Raj, B. Moskowitz, and R. Casciari, "Advances in ferrofluid technology," J. Magn. Magn. Mater. **149**, 174 (1995).
[2] M. Zahn, "Magnetic fluid and nanoparticle applications to nanotechnology," J. Nanopart. Res. **3**, 73 (2001).
[3] F. Sedgemore, "On the brink," Nanomaterials News **3**(7), 05 (2007).
[4] J. Liu, Y. Mao, and J. Ge, "The magnetic assembly of polymer colloids in a ferrofluid and its display applications," Nanoscale **4**, 1598 (2012).
[5] M. Mohammadi, M. Mohammadi, and M. B. Shafii, "Experimental investigation of a pulsating heat pipe using ferrofluid (magnetic nanofluid)," J. Heat Transfer **134**, 014504 (2012).
[6] S. Chaudhari, S. Patil, R. Zambare, and S. Chakraborty, "Exploration on use of ferrofluid in power transformers," in *Proceedings of the 2012 IEEE 10th International Conference on the Properties and Applications of Dielectric Materials, 24 July 2012*, Bangalore, India.
[7] S. Odenbach, "Recent progress in magnetic fluid research," J. Phys. Condens. Matter **16**, R1135 (2004).
[8] K. S. Lok, Y. C. Kwok, P. P. F. Lee, and N.-T. Nguyen, "Ferrofluid plug as valve and actuator for whole-cell PCR on chip," Sens. Actuators B **166–167**, 893 (2012).
[9] J. Dahler and L. E. Scriven, "Angular momentum of continua," Nature (London) **192**, 36 (1961).
[10] D. W. Condiff and J. S. Dahler, "Fluid mechanical aspects of antisymmetric stress," Phys. Fluids **7**, 842 (1964).

[11] R. E. Rosensweig, *Ferrohydrodynamics* (Dover, Mineola, NY, 1997).
[12] R. Moskowitz and R. E. Rosensweig, "Nonmechanical torque-driven flow of a ferromagnetic fluid by an electromagnetic field," Appl. Phys. Lett. **11**, 301 (1967).
[13] R. E. Rosensweig, J. Popplewell, and R. J. Johnston, "Magnetic fluid motion in rotating field," J. Magn. Magn. Mater. **85**, 171 (1990).
[14] R. Brown and T. S. Horsnell, "The wrong way round," Electr. Rev. **184**, 235 (1969).
[15] A. V. Lebedev and A. F. Pschenichnikov, "Rotational effect: The influence of free or solid moving boundaries," J. Magn. Magn. Mater. **122**, 227 (1993).
[16] V. M. Zaitsev and M. I. Shliomis, "Entrainment of ferromagnetic suspension by a rotating field," J. Appl. Mech. Tech. Phys. **10**, 696 (1969).
[17] I. Ya. Kagan, V. G. Rykov, and E. I. Yantovskii, "Flow of a dielectric ferromagnetic suspension in a rotating magnetic field," Magnetohydrodynamics **9**, 258 (1973).
[18] O. A. Glazov, "Motion of a ferrosuspension in rotating magnetic fields," Magnetohydrodynamics **11**, 140 (1975).
[19] O. A. Glazov, "Role of higher harmonics in ferrosuspension motion in a rotating magnetic field," Magnetohydrodynamics **11**, 434 (1975).
[20] S. Feng, A. L. Graham, J. R. Abbott, and H. Brenner, "Antisymmetric stresses in suspensions: Vortex viscosity and energy dissipation," J. Fluid Mech. **563**, 97 (2006).
[21] R. E. Rosensweig and R. J. Johnston, "Aspects of magnetic fluid flow with nonequilibrium magnetization," in *Continuum Mechanics and its Applications*, edited by G. A. C. Graham, and S. K. Malik (Hemisphere, New York, 1989), pp. 707–729.
[22] C. Rinaldi, J. H. Lee, A. D. Rosenthal, T. Franklin, and M. Zahn, "Ferrohydrodynamics in time-varying magnetic fields," in *Proceedings of the IMECE 2002, 17–22 November 2002*, New Orleans, see http://proceedings.asmedigitalcollection.asme.org/proceeding.aspx?articleid=1582354.
[23] A. Chaves, C. Rinaldi, S. Elborai, X. He, and M. Zahn, "Bulk flow in ferrofluids in a uniform rotating magnetic field," Phys. Rev. Lett. **96**, 194501 (2006).
[24] K. P. Travis and D. J. Evans, "Molecular spin in a fluid undergoing Poiseuille flow," Phys. Rev. E **55**, 1566 (1997).
[25] A. Chaves, M. Zahn, and C. Rinaldi, "Spin-up flow of ferrofluids: Asymptotic theory and experimental measurements," Phys. Fluids **20**, 053102 (2008).
[26] S. Khushrushahi and M. Zahn, "Ultrasound velocimetry of ferrofluid spin-up flow measurements using a spherical coil assembly to impose a uniform rotating magnetic field," J. Magn. Magn. Mater. **323**, 1302 (2011).
[27] I. Torres-Diaz, C. Rinaldi, S. Khushrushahi, and M. Zahn, "Observations of ferrofluid flow under a uniform rotating magnetic field in a spherical cavity," J. Appl. Phys. **111**, 07B313 (2012).
[28] M. I. Shliomis, T. P. Lyubimova, and D. V. Lyubimov, "Ferrohydrodynamics: An essay on the progress of ideas," Chem. Eng. Commun. **67**, 275 (1988).
[29] A. F. Pshenichnikov, A. V. Lebedev, and M. I. Shliomis, "On the rotational effect in nonuniform magnetic fluids," Magnetohydrodynamics **36**, 275 (2000).
[30] B. U. Felderhof, "Steady-state hydrodyamics of a viscous incompressible fluid with spinning particles," J. Chem. Phys. **135**, 234901 (2011).
[31] B. U. Felderhof, "Entrainment by a rotating magnetic field of a ferrofluid contained in a sphere," Phys. Rev. E **84**, 046313 (2011).
[32] B. U. Felderhof, "Entrainment by a rotating magnetic field of a ferrofluid contained in a cylinder," Phys. Rev. E **84**, 026312 (2011).
[33] B. A. Finlayson, "Modeling a ferrofluid in a rotating magnetic field," in *Proceedings of the Comsol Conference, October, Boston, 2007*; see http://www.comsol.com/papers/3204/; accessed July 3, 2012.
[34] K. R. Schumacher, In. Sellien, G. S. Knoke, T. Cader, and B. A. Finlayson, "Experiment and simulation of laminar and turbulent ferrofluid pipe flow in an oscillating magnetic field," Phys. Rev. E **67**, 026308 (2003).
[35] M. I. Shliomis, "Effective viscosity of magnetic suspensions," Sov. Phys. JETP **34**, 1291 (1972).
[36] J. A. Osborn, "Demagnetizing factors of the general ellipsoid," Phys. Rev. **67**, 351 (1945).
[37] See supplementary material at http://dx.doi.org/10.1063/1.4812295 for Figures S1–S3.
[38] I. Torres-Diaz and C. Rinaldi, "Ferrofluid flow in the annular gap of a multipole rotating magnetic field," Phys. Fluids **23**, 082001 (2011).